Journal of Computational Applied Mechanics 2023, 54 (1): 140-149
DOI: 10.22059/jcamech.2022.352395.785

RESEARCH PAPER

Sensitivity Analysis of the Finite Element Model of the Foot and Ankle Complex for Vibration Analysis

Laleh Fatahi *, Mohammadhossein Nabgan

Department of Mechanical Engineering, Engineering Faculty, Shahid Chamran University of Ahvaz, Ahvaz, Iran

Abstract

Biomechanical simulation and analysis of human organs are of paramount importance for improving the treatment and prevention of a variety of disorders and injuries. One of the organs that is very prone to injuries, especially among athletes and active individuals, is the foot. However, these injuries can be well-prevented by numerical modeling and analysis of the foot in different conditions. In the current study, after constructing a detailed parametric finite element (FE) model of the foot and ankle complex, a surrogate-based sensitivity analysis is performed to evaluate how the material and geometric properties of the bones, the ligaments, the soft tissue, and the skin affect the natural frequencies of the FE model. Based on the obtained results, Young's modulus and the density of the cortical bone, the trabecular bone and the soft tissue have considerable effects on the natural frequencies. Also, Poisson's ratio of the soft tissue and the thickness of the skin have significantly larger sensitivity indices compared to those of other similar parameters. The cross-sectional area of the fascia plantar also plays a more important role in the natural frequencies compared to those of other ligaments. These results are preliminary good indicators to rank the material and geometrical parameters based on their effects on the natural frequencies of the FE model.

Keywords: Foot and Ankle Complex; Finite Element Method; Mechanical Vibrations; Surrogate Modeling; Sensitivity Analysis

1. Introduction

In the recent decades, the collaborations in the fields of medicine and engineering have significantly increased the understanding of biological systems. Numerical modeling and analysis of human organs have also been the focus of many researchers to better describe the mechanism of a variety of disorders and injuries and enhance the treatments. One of the organs that is highly prone to injuries, especially among athletes and active individuals, is the foot [3]. Numerical modeling and analysis of the foot in different conditions can help clinicians to better treat foot disorders [1], [2]. Vibration therapy [4] is a widely used technique that utilizes vibrations as a physical tool for the treatment of a variety of diseases including those of the foot and ankle complex [5]–[7]. Using an accurate numerical vibration model of the foot can be a good asset to investigate the efficiency of the vibration treatments before applying to the patients. Therefore, an accurate and efficient numerical model is needed for practical purposes. To have a trade-off between the accuracy and the computational costs, one should determine how many details should be considered in the geometric modeling of the organ and how much accuracy is required about the material properties. Morales-Orcajo et al. [8] reviewed a variety of computational models of the human foot including 2D and 3D, detailed and simplified, partial and full-shape models of the lower limb, ankle and foot. The detailed 3D geometric models of the foot are usually obtained from medical imaging scans and image processing techniques [9]. The material properties are usually estimated by performing in vivo and in vitro tests on the organs [10]. The geometrical and material data are then utilized in the numerical models to perform a variety of in silico analyses [11].

In the current research, a detailed 3D finite element model of the foot and ankle complex including the skin, the soft tissue, the cortical and the trabecular bones and the ligaments are constructed for vibration analysis of the foot. To investigate how the uncertainties in the geometric and material properties of the foot tissues affect the natural frequencies of the FE model, a surrogate-based sensitivity analysis is performed. The results can help us to investigate how the

* Corresponding author. Tel.: +98-613-322-6600; fax: +98-613-333-6642; e-mail: lfatahi@scu.ac.ir

uncertainty in the material and geometric parameters influence the vibration response. What follows describes the finite element modeling and modal analysis of the foot and ankle complex that is required in the surrogate modeling and the sensitivity analysis.

2. Finite element modeling and modal analysis of the foot and ankle complex

To construct a detailed FE model of the foot and ankle complex, the geometry of the bones, the soft tissue, and the skin are imported into ANSYS workbench. As shown in Figure (1), the foot has 28 bones, including 14 phalanges (distal, middle, and proximal phalanges), five metatarsals, and seven tarsal bones including the talus, the calcaneus, the cuboid, the navicular, and three cuneiforms (medial, intermediate, and lateral) and two sesamoids. In Figure (2), the finite element of the foot and ankle complex is shown. Note that, each bone consists of a cortical segment, meshed by shell elements and a trabecular segment that is meshed by solid elements (See Figure (2)). The skin and the soft tissue are also meshed with the shell and solid elements, respectively. The ligaments, as listed in Table (1) and graphically shown in Figure (3), are modeled with cable elements to take into account their tension-only behavior. After meshing all the geometries, the FE model consists of 71334 nodes and 58925 elements. It should be noted that since the constructed FE model is used for the linear modal analysis, the material and contact models should be linear ones. To this end, all the contacts of the FE model are considered bonded. The isotropic linear elasticity is also used to describe the stiffness of the tissues.

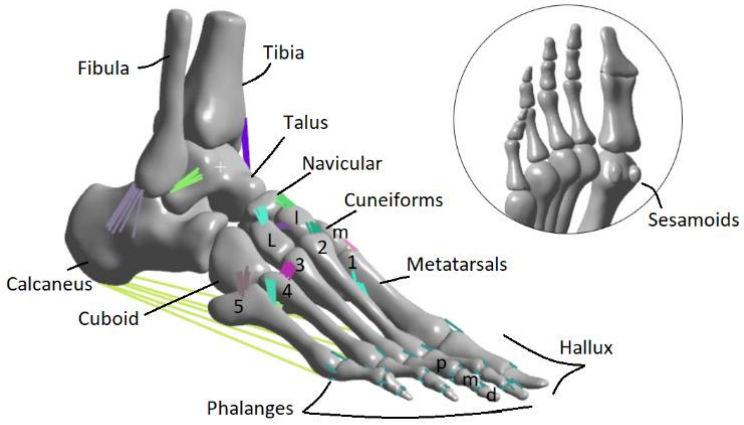

Figure 1. The bones of the foot and ankle complex

Table 1. The ligaments of the foot and ankle complex [13]

Ligament Description	Acronym	No.
Anterior Talofibular Ligament	ATFL	5
Anterior Tibiotalar Ligament	ATTL	6
Calcaneofibular Ligament	CFL	6
Dorsal Cuboid Fifth-Metatarsal	DCbM5	6
Dorsal First-Cuneiform First-Metatarsal	DC1M1	6
Dorsal Fourth-Metatarsal Fifth-Metatarsal	DM4M5	5
Dorsal Second-Cuneiform Second-Metatarsal	DC2M2	6
Dorsal Second-Cuneiform Navicular	DC2Nv	6
Dorsal Third-Metatarsal Fourth-Metatarsal	DM2M4	6
Inferior Calcaneonavicular	ICN	7
Interosseous First-Metatarsal Second-Metatarsal	IM1M2	6
Interosseous Fourth-Metatarsal Fifth-Metatarsal	IM4M5	7
Interosseous Second-Cuneiform Third-Cuneiform	IC2C3	6
Interosseous Third-Cuneiform Cuboid	IC3Cb	6
Medial First-Cuneiform First-Metatarsal	MC1M1	6
Plantar First-Cuneiform First-Metatarsal	PC1M1	6
Posterior Talofibular Ligament	PTFL	6
Posterior Tibiotalar Ligament	PTTL	6
Short Plantar Ligament	SPL	6

Tibiocalcaneal Ligament	TCL	6

The material and geometric parameters of the FE model are tabulated in Table (2). Note that the initial values of these parameters were obtained from the available literature [3], [13] and the FE model is parameterized to be used in the sensitivity analysis. Regarding the boundary condition of the FE model, only the displacements on the top surface of the tibia, the fibula, and the soft tissue are prohibited. Note that the current FE model is aimed to be used in the future research dealing with vibration therapy of the foot and ankle. Since the vibration treatments are usually in a lying or sitting position, the mass of the upper body is not employed in the current FE model.

To extract the modal parameters of the FE model, an eigenvalue problem is solved. The first four natural frequencies under 100 Hz and their corresponding mode shapes are reported in Figure (4) and utilized in the sensitivity analysis. Note that, as mentioned before, the soft tissue and the skin are included in the FE model of the foot and ankle complex, however, they are hidden in Figure (4) to show the displacements of the bones.

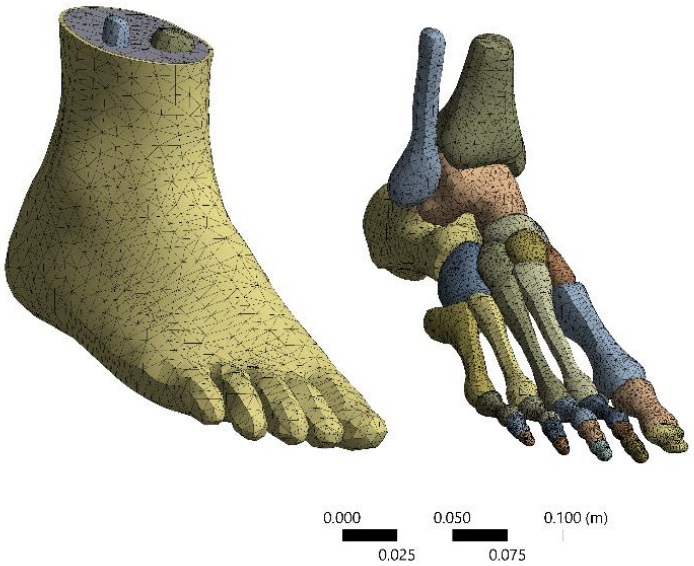

Figure 2. The finite element model of the foot and ankle complex

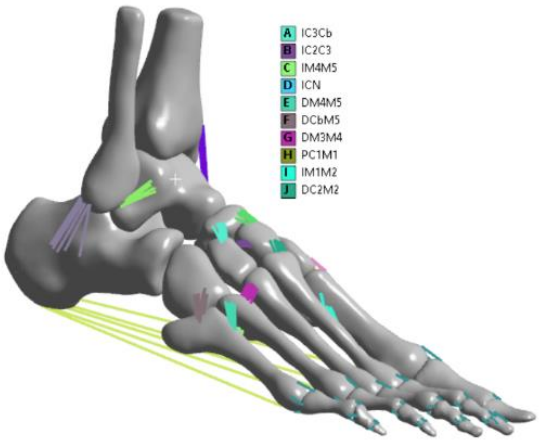

Figure 3. The ligaments of the FE model of the foot and ankle complex

3. Surrogate Modeling

Surrogate modeling is an engineering approach that can be utilized when a direct evaluation of the output of a numerical model is computationally prohibitive, especially when an interactive procedure should be performed on the FE model. The surrogate modeling aims to select the design points that can extract maximum information about the output of the FE model. After the selection of the design points, also known as the design of experiment approach, a surface is fitted on the design points in a way that the best possible approximation to the output of the FE model is obtained. The fitted surfaces should match the FE model at least in a small vicinity of the surface [14]. In the current research, the optimal space-filling design is used to find the proper design points. In this method, the design points are placed in the design domain so that they have the farthest possible distance [15]. To this end, first, the minimum distance between the design points is found, then, this distance is maximized, this is why this approach is also called the maximin

distance design [16]. Moreover, to fit a surface on the design points, the Kriging method [17] is utilized in this research in which a curve is fitted on the design points based on the regression analysis.

4. Surrogate-based sensitivity analysis

To investigate the effect of the uncertainties in the material and geometric parameters of the FE model, a sensitivity analysis is performed. As mentioned before, to reduce the computational costs, a surrogate-based sensitivity analysis is utilized where the design points are created using the optimal-space filling design, and a response surface is fitted on the design points using the Kriging method. The material parameters including the density, Young's modulus and Poisson's ratio of the different tissues as well as the geometric parameters including the thickness of cortical bones and the radius of the circular cross-section of the cable elements are considered as design parameters. The list of these parameters is tabulated in Table (2). It is assumed that each design parameter can vary by ±5 percent of its initial value. A local sensitivity index is then evaluated based on the variation of the natural frequencies as the design parameter varies from its lower bound to its upper bound, while the other design parameters are kept constant.

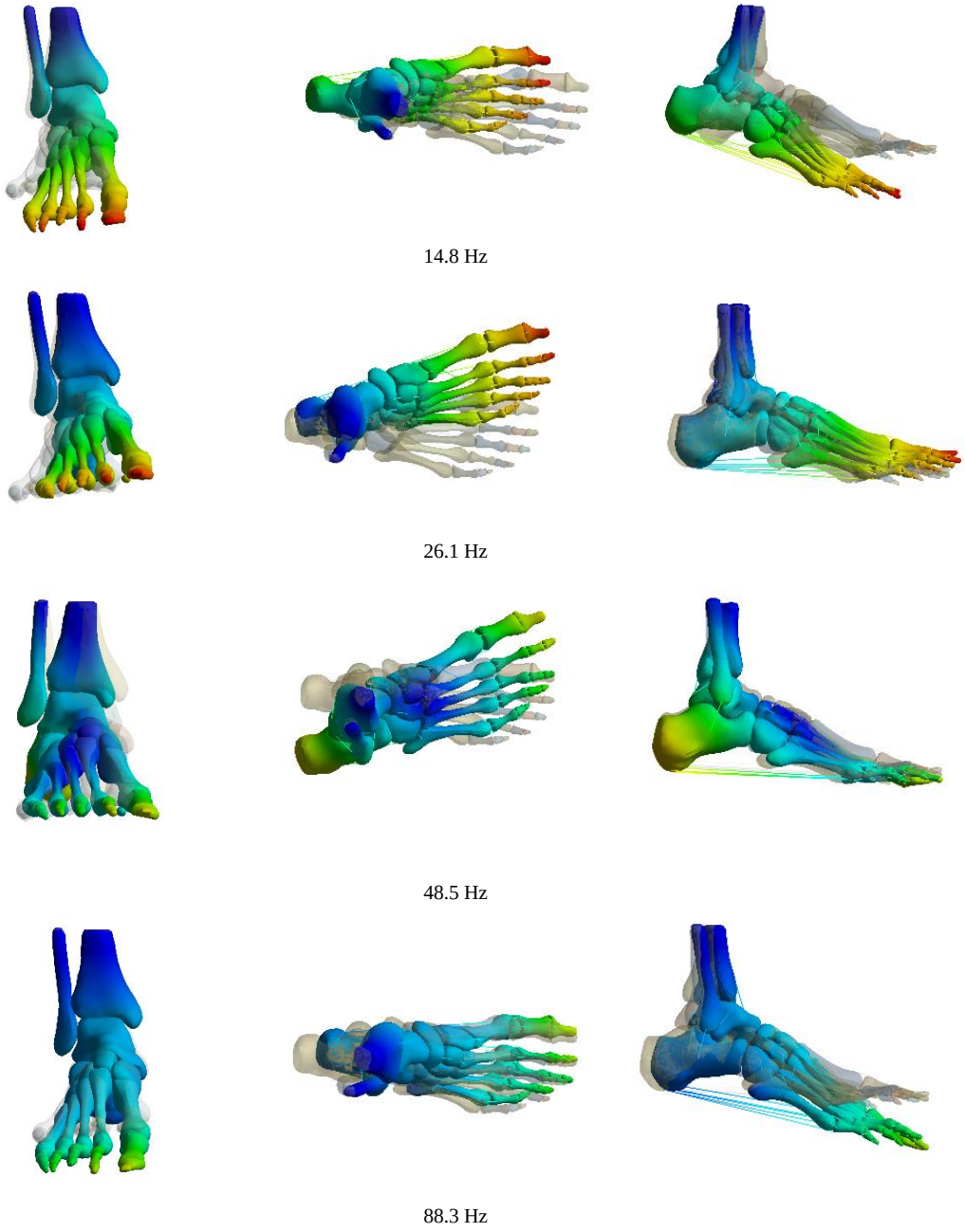

Figure 4. The first four natural frequencies and the corresponding mode shapes of the FE model of the foot and ankle complex

(left) front view (middle) top view (right) side view

Table 3. The material and the geometric parameters of the FE model

Description	Symbol (Unit)	Initial Value
Density of trabecular bones	ρ1 (Kg/m^3)	1990
Density of cortical bones	ρ2 (Kg/m^3)	1990
Density of fascia plantar	ρ3 (Kg/m^3)	1000
Density of ligaments	ρ4 (Kg/m^3)	1000
Density of skin	ρ5 (Kg/m^3)	950
Density of soft tissue	ρ6 (Kg/m^3)	950
Young's modulus of trabecular bones	E1 (MPa)	0.40
Young's modulus of cortical bones	E2 (MPa)	17000
Young's modulus of fascia plantar	E3 (MPa)	350
Young's modulus of ligaments	E4 (MPa)	265
Young's modulus of skin	E5 (MPa)	0.45
Young's modulus of soft tissue	E6 (MPa)	0.45
Poisson's ratio of trabecular bones	v1	0.3
Poisson's ratio of cortical bones	v2	0.3
Poisson's ratio of skin	v3	0.45
Poisson's ratio of soft tissue	v4	0.45
Thickness of the cortical bones	t1-26 (mm)	1.00
Thickness of the skin	t27(mm)	2.00
Radius of IC3Cb ligament	R1 (mm)	7.57
Radius of IC2C3 ligament	R2 (mm)	6.63
Radius of IM4M5 ligament	R3 (mm)	5.19
Radius of ICN ligament	R4 (mm)	7.50
Radius of DM4M5 ligament	R5 (mm)	4.30
Radius of DCbM5 ligament	R6 (mm)	50
Radius of DM3M4 ligament	R7 (mm)	3.50
Radius of PC1M1 ligament	R8 (mm)	4.30
Radius of IM1M2 ligament	R9 (mm)	4.70
Radius of DC2M2 ligament	R10 (mm)	3.30
Radius of DC2Nv ligament	R11 (mm)	3.78
Radius of ATFL ligament	R12 (mm)	4.70
Radius of DC1M1 ligament	R13 (mm)	3.10
Radius of SPL ligament	R14 (mm)	5.75
Radius of PTTL ligament	R15 (mm)	5.60
Radius of MC1M1 ligament	R16 (mm)	3.64
Radius of ATTL ligament	R17 (mm)	4.00
Radius of PTFL ligament	R18 (mm)	4.20
Radius of TCL ligament	R19 (mm)	4.60
Radius of CFL ligament	R20 (mm)	2.73
Radius of MTP ligament	R21 (mm)	3.00
Radius of FASCIA Plantar	R22 (mm)	3.10

5. Results and discussions

After constructing the design sets using the optimal-space filling design method, the Kriging method is utilized to fit the response surfaces. To investigate the accuracy of the fitted surfaces, the predicted versus the observed natural frequencies are compared. Based on the obtained results, the predicted values of the natural frequencies from the surrogate model and the observed values from the FE model match well, as shown in Figure (5). Note that to show the

charts of the four different natural frequencies in one figure, they are normalized so that in every design set, 0 is assigned to the minimum natural frequency of each mode and 1 is devoted to the maximum natural frequency of that mode.

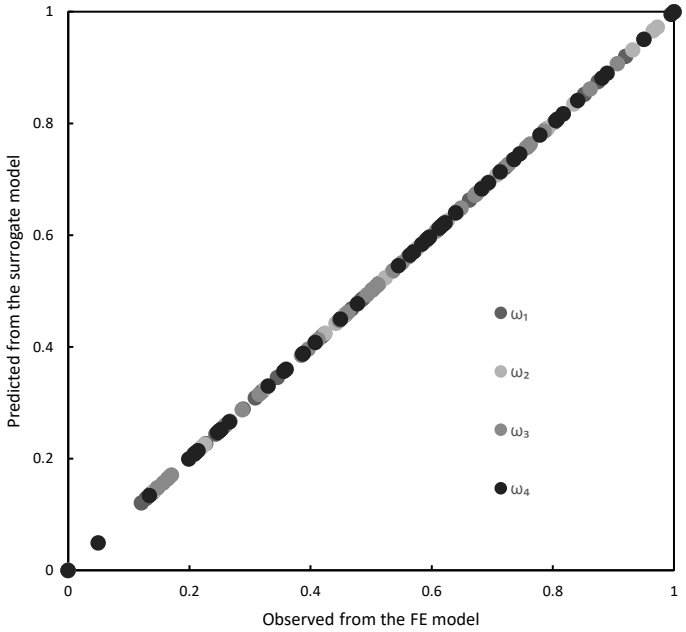

Figure 5. The predicted normalized natural frequencies from the surrogate model vs the observed values from the FE model

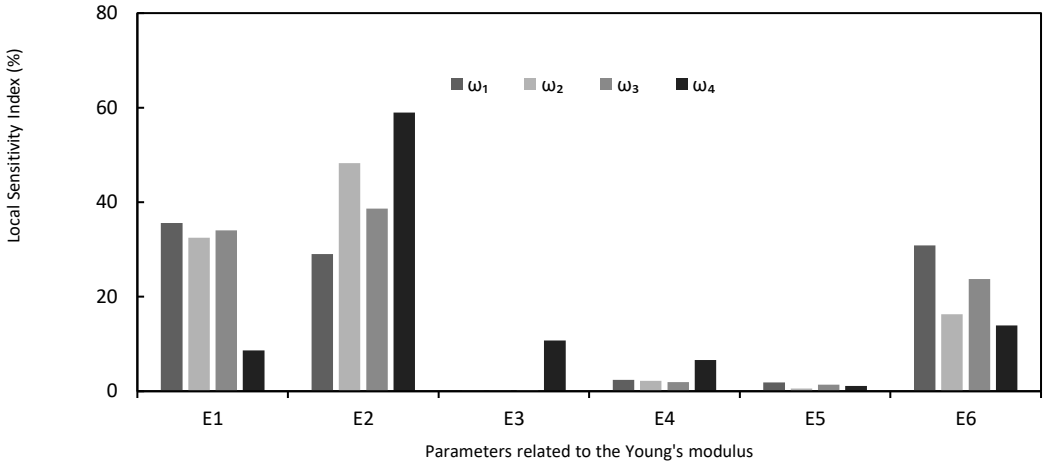

Figure 6. Sensitivity of the natural frequencies to Young's modulus parameters

Based on the results obtained from the sensitivity analysis on the surrogate model, the sensitivity indices of Young's modulus of the trabecular and the cortical bones and the soft tissue are considerably larger than those of the ligaments, the fascia, and the skin (See Figure (6)). Among the density parameters, those of the soft tissue and the trabecular bones have the largest sensitivity indices while the density of the ligaments and the skin have smaller indices as depicted in Figure (7). The sensitivity indices of Poisson's ratio of the soft tissue, as observed in Figure (8), is significantly higher than those of other similar parameters. Regarding the thickness parameters, as shown in Figure (9), it is seen that the thickness of the skin and the cortical thickness of the tibia, the fibula, the talus, and the metatarsals bones have the largest sensitivity indices while the fourth and fifth phalanges and the cuboid have the smallest ones. Moreover, the effect of the cross-sectional areas of the fascia plantar on the natural frequencies is considerably higher than those of other ligaments (see Figure (10)). It is observed that the smallest sensitivity indices are of the ICN, DC1M1, PTTL, and

MC1M1 ligaments. These results provide preliminary good indicators to rank the material and geometrical parameters based on their effects on the natural frequencies of the FE model.

6. Conclusions

In the current research, a detailed parametric 3D finite element model of the foot and ankle complex is developed to investigate the sensitivity of the natural frequencies to the material and geometric parameters related to the bones, the ligaments, the soft tissue, and the skin. Based on the results obtained from a surrogate-based sensitivity analysis, Young's modulus and the density of the cortical and the trabecular bones as well as the soft tissue have considerable effects on the natural frequencies. Also, Poisson's ratios of the soft tissue and the thickness of the skin have significantly larger sensitivity indices compared to those of other similar parameters. The cross-sectional area of the fascia plantar also plays a more important role in all the natural frequencies compared to those of other ligaments. These results are good indicators to rank the design parameters of the FE model of the foot and ankle complex based on their effects on the natural frequencies.

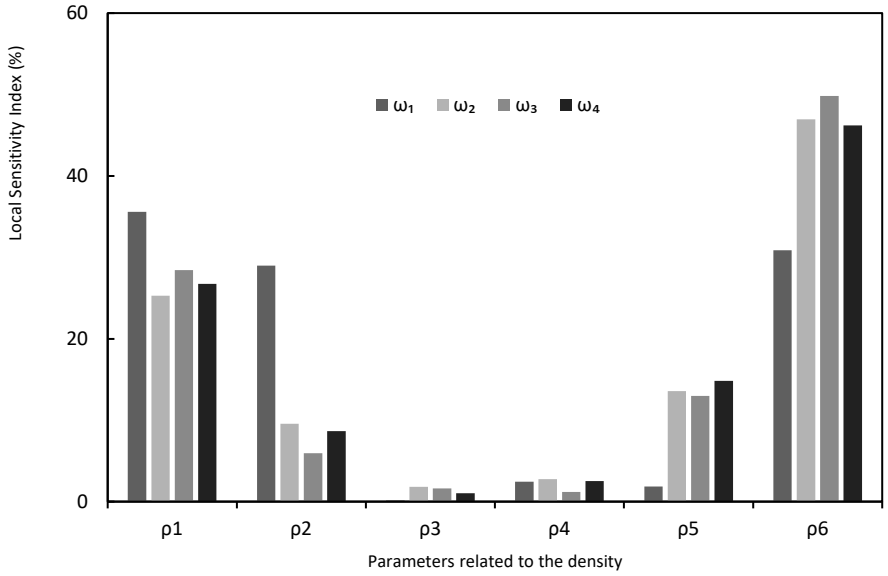

Figure 7. Sensitivity of the natural frequencies to the density parameters

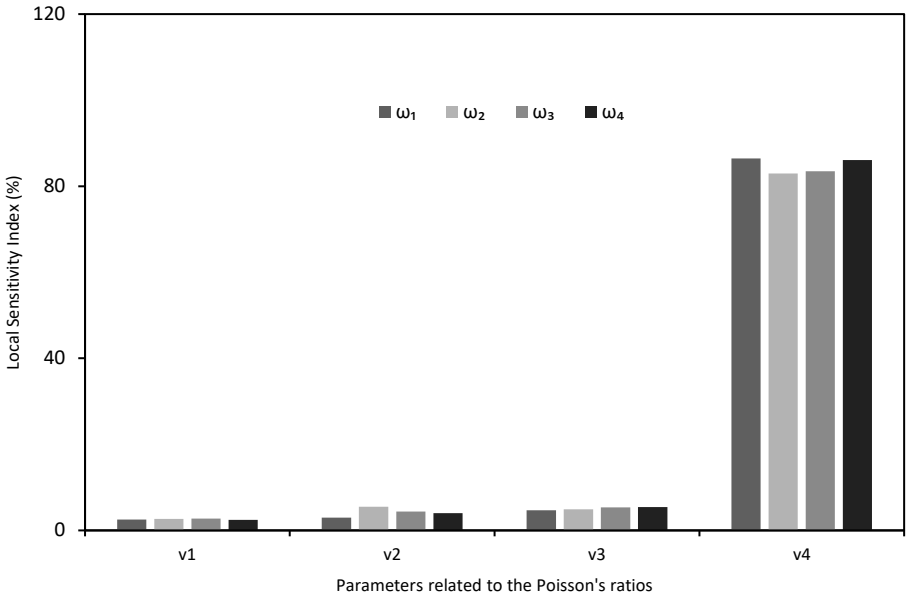

Figure 8. Sensitivity of the natural frequencies to Poisson's ratios

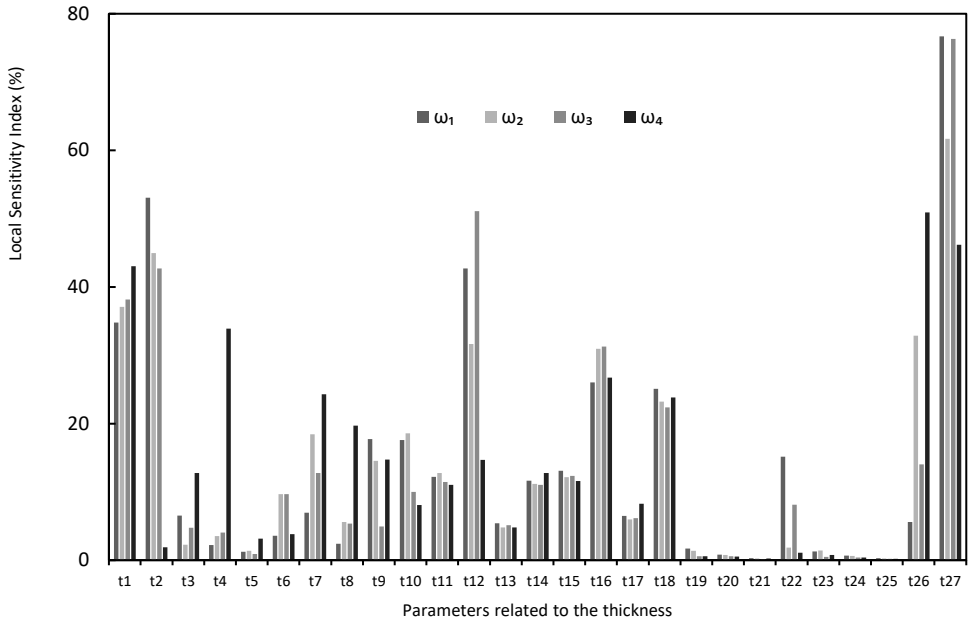

Figure 9. Sensitivity of the natural frequencies to the thickness parameters of the bones and skin

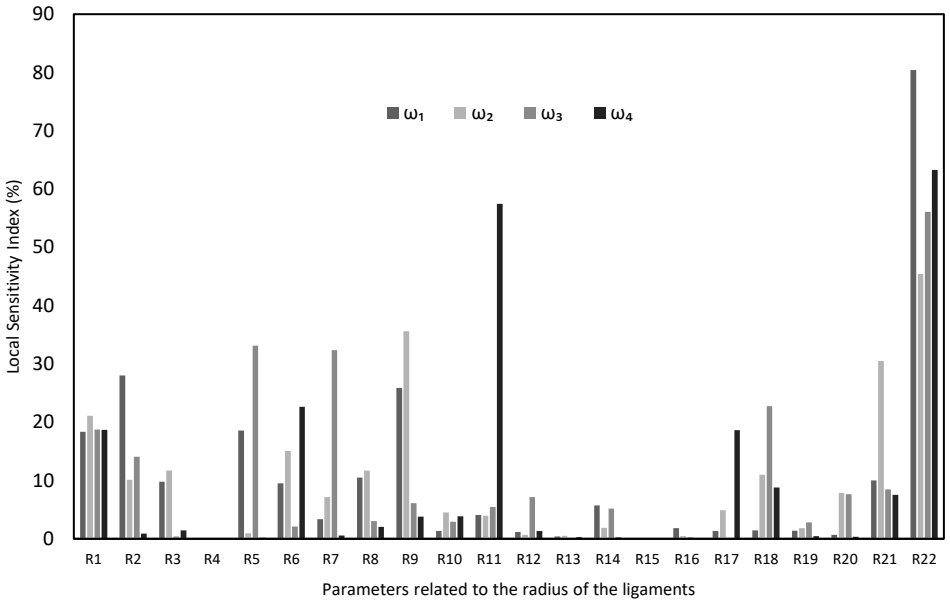

Figure 10. Sensitivity of the natural frequencies to the parameters related to the radius of the ligaments

References

[1] Y. Wang, D. W.-C. Wong, and M. Zhang, "Computational models of the foot and ankle for pathomechanics and clinical applications: a review," *Ann. Biomed. Eng.*, vol. 44, no. 1, pp. 213–221, 2016.

[2] A. M. Takhakh, F. M. Kadhim, and J. S. Chiad, "Vibration Analysis and Measurement in Knee Ankle Foot Orthosis for Both Metal and Plastic KAFO Type," in *ASME International Mechanical Engineering Congress and Exposition*, 2013, vol. 56222, p. V03BT03A050.

[3] M. Zhang and Y. Fan, *Computational biomechanics of the musculoskeletal system*. CRC Press Boca Raton, FL, USA, 2015.

[4] F. Rauch, "Vibration therapy," *Dev. Med. Child Neurol.*, vol. 51, pp. 166–168, 2009.

[5] B. Önal, M. Sertel, and G. Karaca, "Effect of plantar vibration on static and dynamic balance in stroke patients: a randomised controlled study," *Physiotherapy*, vol. 116, pp. 1–8, 2022.

[6] M. Sabziparvar, S. Naghdi, N. N. Ansari, H. R. Fateh, and A. Nakhostin-Ansari, "Local plantar vibration for the treatment of diabetic neuropathy: a case report," *J. Diabetes Metab. Disord.*, vol. 20, no. 2, pp. 2115–2119, 2021.

[7] L. Xie, S.-X. Yi, Q.-F. Peng, P. Liu, and H. Jiang, "Retrospective study of effect of whole-body vibration training on balance and walking function in stroke patients," *World J. Clin. cases*, vol. 9, no. 22, p. 6268, 2021.

[8] E. Morales-Orcajo, J. Bayod, and E. de Las Casas, "Computational foot modeling: scope and applications," *Arch. Comput. Methods Eng.*, vol. 23, no. 3, pp. 389–416, 2016.

[9] S. M. A. Taleghani and L. Fatahi, "Application of Medical Imaging and Image Processing in Creating 3D Models of Human Organs," in *International Conference on Mechanics of Advanced Materials and Equipment*, 2018, pp. 1–10.

[10] X. Ge, L. Zhang, G. Xiang, Y. Hu, and D. Lun, "Cross-Sectional Area Measurement Techniques of Soft Tissue: A Literature Review," *Orthop. Surg.*, vol. 12, no. 6, pp. 1547–1566, 2020.

[11] P. K. Phan *et al.*, "In Silico Finite Element Analysis of the Foot Ankle Complex Biomechanics: A Literature Review," *J. Biomech. Eng.*, vol. 143, no. 9, 2021.

[12] H. Ou, Z. Qaiser, L. Kang, and S. Johnson, "Effect of skin on finite element modeling of foot and ankle during balanced standing," *J. Shanghai Jiaotong Univ.*, vol. 23, no. 1, pp. 132–137, 2018.

[13] C. Mkandawire, W. R. Ledoux, B. J. Sangeorzan, and R. P. Ching, "Foot and ankle ligament morphometry," *J. Rehabil. Res. Dev.*, vol. 42, no. 6, p. 809, 2005.

[14] R. H. Myers, D. C. Montgomery, and C. M. Anderson-Cook, *Response surface methodology: process and product optimization using designed experiments*. John Wiley & Sons, 2016.

[15] V. R. Joseph, "Space-filling designs for computer experiments: A review," *Qual. Eng.*, vol. 28, no. 1, pp. 28–35, 2016.

[16] M. E. Johnson, L. M. Moore, and D. Ylvisaker, "Minimax and maximin distance designs," *J. Stat. Plan. Inference*, vol. 26, no. 2, pp. 131–148, 1990.

[17] T. J. Santner, B. J. Williams, W. I. Notz, and B. J. Williams, *The design and analysis of computer experiments*, vol. 1. Springer, 2003.